

Article

Identification for Abutment Stress by Drilling Cuttings

Jian Tan ^{1,*}, Yunliang Tan ^{2,3}, Zihui Wang ^{2,3} and Yubao Zhang ^{2,3} 

¹ School of Information and Control Engineering, China University of Petroleum, China University of Petroleum(East China), Qingdao 266580, China

² State Key Laboratory of Mining Disaster Prevention and Control Cofounded by Shandong Province and the Ministry of Science and Technology, College of Energy and Mining Engineering, Shandong University of Science and Technology, Qingdao 266590, China; yunliangtan@163.com (Y.T.); wangzihui1234@163.com (Z.W.); yubao.zhang@sdust.edu.cn (Y.Z.)

³ College of Energy and Mining Engineering, Shandong University of Science and Technology, Qingdao 266590, China

* Correspondence: tjy111p@126.com

Abstract: The concentration of abutment pressure acting on coal seams induced by mining is a key factor to trigger rock burst. Understanding of abutment pressure or stress concentration is fundamental in preventing and controlling rock burst. The influence on abutment pressure fluctuation caused by the inhomogeneity of coal seams needs to be considered, but it is difficult to obtain by the present usual ways such as acoustic transmission, electromagnetic wave transmission, etc. In this article, the relationship between the amount of cuttings drilled in a coal seam and stress level was analyzed by considering the effect of drilling cutting expansion, and the drilling cutting test was carried out in Xinglongzhuang Coal Mine, Shandong Energy Ltd. It is found that the amount of cuttings drilled is positively related to the degree of stress concentration in both the plastic fracture zone and elastic zone. The amount of drilling cuttings is closely related to the roof weighting. In addition, the irregular fluctuation of drilling cuttings is an approximate map of distribution of stress concentration because of the non-uniformity of cracks and other defects in the coal seam. In order to meet the need of rock burst prevention by accurate pressure relief in high-stress zones, enough boreholes are needed.

Keywords: abutment stress; drilling cutting; roof weighting; pressure relief



Citation: Tan, J.; Tan, Y.; Wang, Z.; Zhang, Y. Identification for Abutment Stress by Drilling Cuttings. *Appl. Sci.* **2021**, *11*, 9467. <https://doi.org/10.3390/app11209467>

Academic Editor:
Giuseppe Lacidogna

Received: 5 August 2021
Accepted: 4 October 2021
Published: 12 October 2021

Publisher's Note: MDPI stays neutral with regard to jurisdictional claims in published maps and institutional affiliations.



Copyright: © 2021 by the authors. Licensee MDPI, Basel, Switzerland. This article is an open access article distributed under the terms and conditions of the Creative Commons Attribution (CC BY) license (<https://creativecommons.org/licenses/by/4.0/>).

1. Introduction

With the continuous mining of the coal seam, the stress distribution in the coal seam will move forward and change. The vertical stress is called the abutment pressure. The concentration of abutment pressure in the coal seam generally causes serious damage to roadways, even more induces rock burst. Therefore, how to determine abutment pressure distribution has become a hot topic. Generally, analytical and numerical simulations are the commonly used methods in rationale analysis [1]. Vibration wave detection and online stress monitoring are utilized in situ [2,3]. However, because of the complexity of different scale fissures or cracks in the coal seam structure and the influence of roof movement, the detection accuracy of abutment pressure and its changes by using vibration wave detection and online stress monitoring should be improved.

As one of the methods for monitoring the danger of rock burst, the drilling cuttings method has been utilized. Its principle is to drill small-diameter holes into coal; the amount of cuttings discharged through a hole per unit length is used to understand the stress concentration. This method was used first in the early 1960s in Germany [4] and then spread to the Soviet Union, Poland and the United Kingdom [5]. In China, drilling cuttings began to be trialed for rock burst early warning in coal mines in 1985 [6,7]. In recent years, many investigations such as early warning threshold determination of drilling cutting amount [8–10], methods of obtaining the evaluation index of drilling

cuttings [11,12], analyses of influencing factors [13,14] and tests of pressure relief effect [15] were done. One successful example is the prediction of rock burst risk in Kaiping Mines, Hebei Province, China, in the early 1980s. The index of drilling powder rate was used to determine the danger level of rock burst. After that, Longfeng Coal Mine in Fushun, China, put forward a method combining drilling cuttings, laboratory experiments and theoretical calculations to determine the grade of shock hazard. Many coal mines in China, such as Mentougou Coal Mine in Beijing, Quantai Coal Mine and Sanhejian Coal Mine in Jiangsu Province, Zaozhuang Mining Bureau and Xinwen Coal Mine in Shandong Province, and Qianqiu Coal Mine in Henan Province have also carried out on-site drilling cuttings monitoring for the prevention of rock burst. As an indicator of stress level, drilling cutting was also used to evaluate gaseous properties of coal and gas stress [16,17]. Much more, the relationship between acoustic emission (AE) signals and diamond drill bit wear was obtained in order to gather and interpret data to allow overall improvement of drilling performance, and through understanding the characteristics of AE signals in terms of the operational parameters of the drilling apparatus, drilling performance was improved [18,19].

Because distribution of abutment pressure or stress concentration is closely related to roof movement, investigating the roof weighting influence on abutment stress changes by drilling cutting is worth doing. This paper intends to analyze the relationship between drilling cuttings amount and the stress firstly, then to investigate the relationship between drilling cuttings and abutment pressure distribution in different stages of roof movement as the coalface advances.

2. Rationale

When the coal seam is drilled, its powder discharge is composed of two parts: one is the pulverized coal formed due to drilling broken with the same borehole diameter, the other is the pulverized coal produced with the action of stress changing around the borehole. The former is only related to pore size, while the latter is related to stress state and mechanical properties of the coal seam and stress state of the surrounding rock. In general, in order to explain the relationship between cuttings amount and stress, the Mohr–Coulomb criterion and the Kastner formula based on the ideal elastoplastic assumption are used [20–22]. Moreover, after strain softening behavior beyond the strength limit is considered, a solution of plane strain of infinite medium with a circular hole based on elastic-plastic assumption is obtained [20].

In an in situ elastic stress zone, a borehole affected by surrounding stress changes, fracture zone, plastic softening zone and elastic zone appear in turn, as shown in Figure 1. The amount of cuttings produced due to elastic displacement of the inner wall is named f_2 . Another part of coal cuttings produced by the plastic-fractured zone and dilatancy is named f_3 , which can be approximated as a linear shape in the plastic-fractured zone.

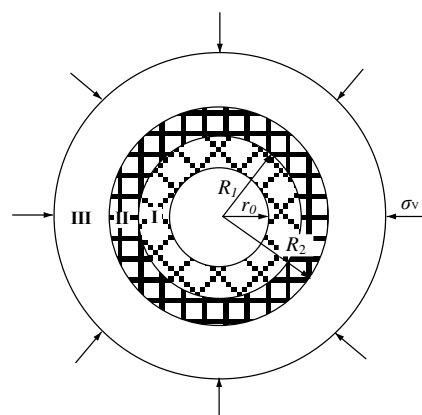


Figure 1. Plane strain borehole model in coal seam. r_0 —Borehole radius, R_1 —Radius of fractured zone, R_2 —Radius of plastic zone, I—Fractured zone, II—Plastic zone, III—Elastic zone.

The amount of drilling cuttings produced by elastic deformation, f_2 , is

$$f_2 = 2\pi r^2 \rho \sigma_v \frac{1 + \mu}{E} \quad (1)$$

where μ is the Poisson's ratio of coal, E is the Young's modulus and σ_v is surround rock stress.

The strain softening constitutive equation of coal is considered as [20]

$$\sigma = \begin{cases} E\varepsilon & (\varepsilon \leq \varepsilon_c) \\ \sigma_c \left(\frac{\varepsilon}{\varepsilon_c}\right)^m & (\varepsilon \geq \varepsilon_c) \end{cases} \quad (2)$$

where m is the plastic softening coefficient, σ_c is the uniaxial compressive strength (MPa) and ε_c is the strain corresponding to the uniaxial compressive strength.

In order to simplify the calculation, the equilibrium equations of plastic and failure zone are the same as follows:

$$\frac{d\sigma_r}{dr} + \frac{\sigma_r - \sigma_\theta}{r} = 0 \quad (3)$$

where σ_r is the radial stress and σ_θ is the tangential stress.

The Mohr–Coulomb criterion is considered as yield condition:

$$\sigma_\theta = q\sigma_r + \sigma_c \quad (4)$$

Considering boundary conditions: when $r = r_0$, $\sigma_r = 0$; when $r = R_2$, the stress must be continuous at the boundary between the elastic and inelastic regions, the inelastic deformation or plastic-fractured R_2 was obtained as follows:

$$R_2 = r_0 \left[1 + \frac{(2m + \xi - 1)(2\sigma_v - \sigma_c)}{\sigma_c^{1-m} [\sigma_c + (\xi - 1)\sigma_v]^m (\xi + 1)} \right]^{\frac{1}{2m + \xi - 1}} \quad (5)$$

where $\xi = \frac{1 + \sin \varphi}{1 - \sin \varphi}$, φ is the internal friction angle.

If the dilatancy effect is not taken into account, the radial displacement at the junction of the inelastic zone and the elastic zone of borehole, u_{R_2} , is

$$u_{R_2} = \frac{1 + \mu}{2E} R_2 \left[\sigma_c + \frac{\xi - 1}{\xi + 1} (2\sigma_v - \sigma_c) \right] \quad (6)$$

The radial displacement of bore wall is easily obtained from the condition that the volume is constant.

$$u_r = \frac{u_{R_2}}{r_0} R_2 \quad (7)$$

When the inelastic deformation of the coal is considered, and the dilatancy coefficient n varies linearly along the radial direction of borehole, as shown in Figure 2, the radial displacement caused by the expansion is

$$\frac{\int_{r_0}^{R_2} 2\pi l \left[\frac{n_1 - 1}{r_0 - R_2} (l - r_0) + n_1 \right] dl - \pi (R_2^2 - r_0^2)}{2\pi r_0} = \frac{(n_1 - 1)(R_2 - r_0)(R_2 + 2r_0)}{6r_0} \quad (8)$$

The radial displacement of the inner wall of the hole including expansion was obtained,

$$u_r = \frac{u_{R_2}}{r_0} R_2 + \frac{(n_1 - 1)(R_2 - r_0)(R_2 + 2r_0)}{6r_0} \quad (9)$$

where u_r is the radial displacement.

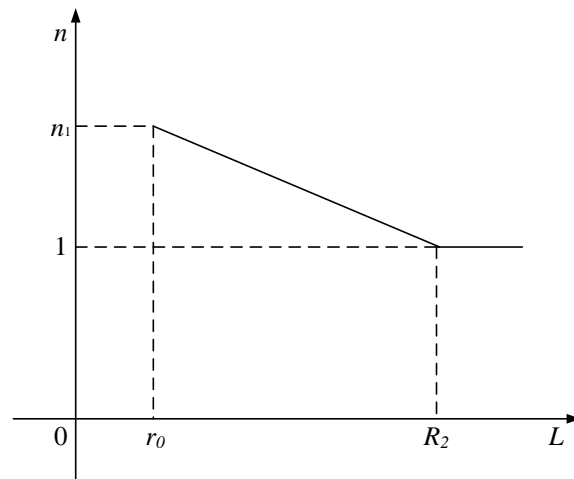


Figure 2. Radial expansion coefficient of borehole.

The amount of cuttings per unit hole length including expansion, S_3 , was derived.

$$\begin{aligned}
 S_3 &= 2\pi r_0 \rho u_r = 2\pi r_0 \rho \left[\frac{u_{R_2}}{r_0} R_2 + \frac{(n_1 - 1)(R_2 - r_0)(R_2 + 2r_0)}{6r_0} \right] \\
 &= 2\pi \rho R_2 u_{R_2} + \frac{1}{3} \pi \rho (n_1 - 1)(R_2 - r_0)(R_2 + 2r_0) \\
 &= \pi \rho R_2^2 \frac{1 + \mu}{E} \left[\sigma_c + \frac{\xi - 1}{\xi + 1} (2\sigma_v - \sigma_c) \right] + \frac{1}{3} \pi \rho (n_1 - 1)(R_2 - r_0)(R_2 + 2r_0)
 \end{aligned}
 \tag{10}$$

Thus, the total amount of cuttings per unit hole length was obtained,

$$S = \rho \pi r_0^2 + S_2 + S_3 \tag{11}$$

where S is the total amount of cuttings.

As mentioned above, the amount of cuttings is approximately positively correlated with the confining pressure; it can be regarded as a measure of the equivalent stress. This was verified in Xinglongzhuang Coal Mine, as shown in Figure 3.

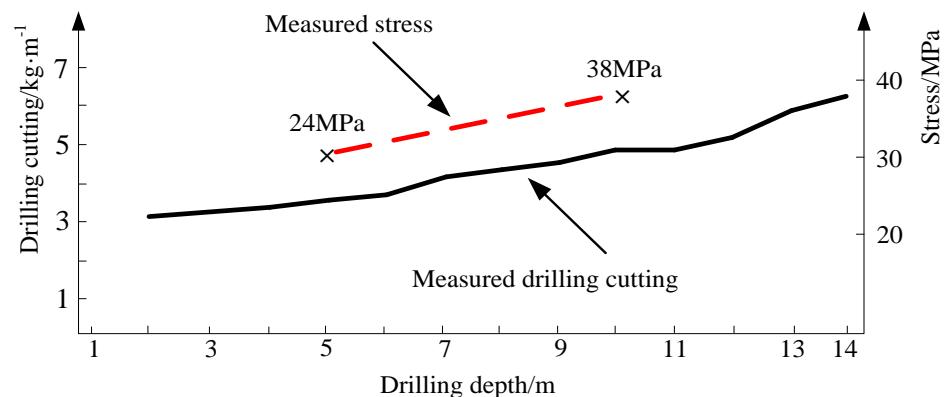


Figure 3. Comparison of measured drilling cutting and measured stress in Xinglongzhuang Coal Mine.

3. In Situ Investigation

3.1. Geologic and Mining Conditions

In order to obtain the relationship between roof movement and equivalent stress or drilling cuttings amount, the trial site was selected in the No. 10304 working face of Xinglongzhuang Coal Mine, Shandong Energy Ltd. The trial working face is located in the middle region of the 10th section, as shown in Figure 4.

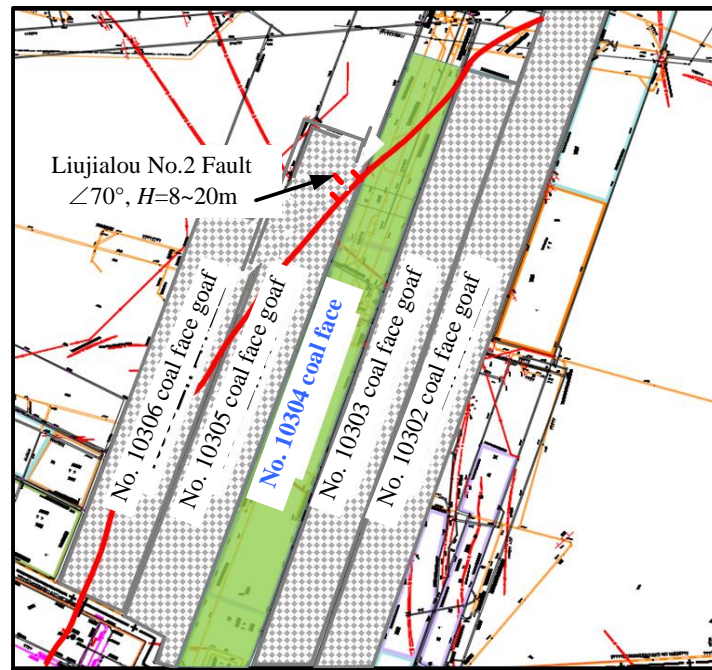


Figure 4. The location of No. 10304 working face.

The coal seam numbered as No. 10 is 8.8 m in average thickness. The strike length and the incline length of the coalface are 2370 and 211 m, respectively. The mining depth is 470 m, the uniaxial strength of coal is 19.34 MPa, Young’s Modulus is 38.62 MPa and density is $1.436 \times 10^4 \text{ KN/m}^3$. When the trial work began, the coalface had been extracted 1661 m from east to west in orientation. Its north side is adjacent to No. 10303 goaf and south side is adjacent to No. 10305 goaf, as shown in Figure 5.

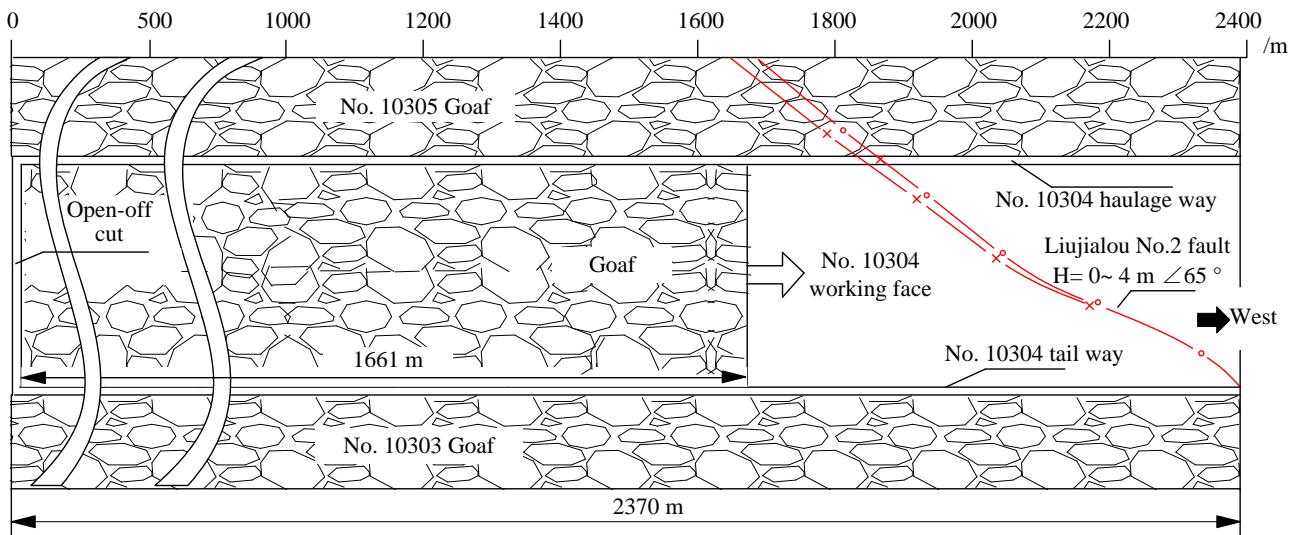


Figure 5. Working face layout plan.

The roof above the seam consists of three layers. The first layer is 2.4 m thick fine slit sandstone with scattered beddings; it is called the immediate roof. The second layer is 11.5 m thick medium-grained sandstone; it is called the lower main roof. The third layer is 22.6 m thick interbedded sandstone; it is called the upper main roof, as shown in Figure 6.

Rock strata	Lithology	Thickness/m	Histogram
Main roof	Sandstone interbedding	22.6	
	Medium grained sandstone	11.5	
Immediate roof	Siltstone	2.4	
Coal seam	Coal	8.8	

Figure 6. Lithology section.

3.2. Drilling Arrangement

For the sake of investigation of stress concentration and changes in the coal seam as the coalface advances, a number of boreholes with 42 mm diameter were drilled along the coal wall in No. 10304 tail way. Borehole drilling is located near the center of the wall in the direction altitude. In order to meet the need of pressure relief for rock burst prevention at the same time, the trial stations were arranged 15, 45, 75 and 105 m away from the working face, separately. Every hole length is 14 m, as shown in Figure 7. Drillings were performed once a day, and cuttings were collected to be weighed out in time. Drilling works were moved forward in turn with the advance of the working face. The drilling jobs were begun at the location where the coalface is 1661 m long from the initial cut way, while the roof is in a stable stage.

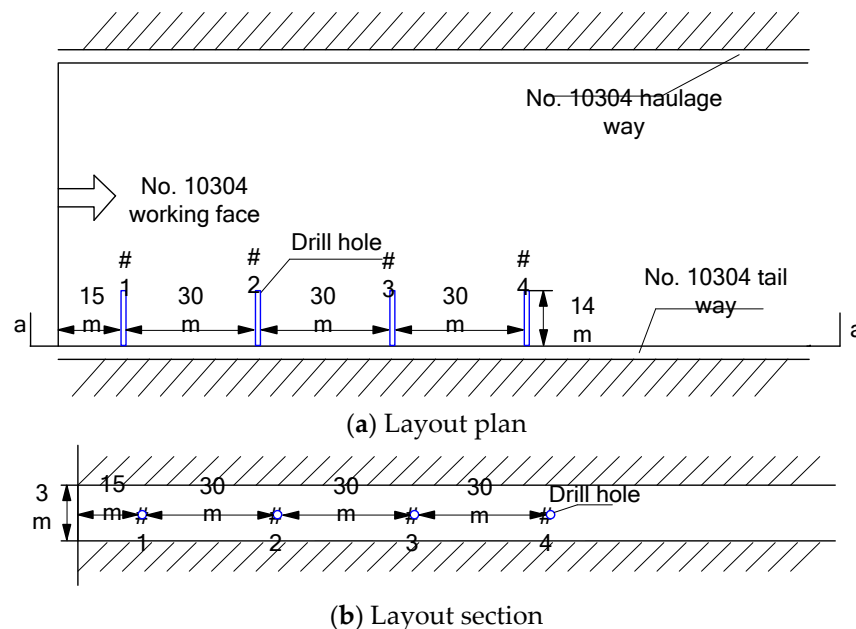


Figure 7. Layout of drilling holes in No. 10304 tail way.

ZQS series pneumatic hand-held drilling machines, manufactured by Hebei Chuanan Coal Mine Machinery Manufacturing Co. Ltd., were used to drill. Drilling performed for powder was in accordance with China’s national standards: Methods for test, monitoring and prevention of rock burst—Part 6: Monitoring method of drilling bits (GB/t 25217.6-2019) [8]. For each 1 m length borehole drilling, the cut coal powder in the hole was taken out. After it was weighed, the change in cuttings with drilling length could be analyzed.

3.3. Data Processing

The Thin Plate Spline (TPS) was used to smooth the difference of drilled powder variation in different places and depths. The rationale can be described as follows: suppose there are n sets of points in the region of Space R^2 , i.e., $P_i, i = 1, 2, \dots, n$; their coordinates are expressed as $(x_i, y_i, z(x_i, y_i))$. If $Z(x_i, y_i)$ has a quadratic continuous derivative, then the energy function can be represented as

$$E = \iint_{R^2} \left[\left(\frac{\partial^2 z}{\partial^2 x} \right)^2 + 2 \left(\frac{\partial^2 z}{\partial x \partial y} \right)^2 + \left(\frac{\partial^2 z}{\partial^2 y} \right)^2 \right] dx dy \quad (12)$$

For TPS problem, it can be solved by minimizing the energy function:

$$Z_{\text{tps}} = \arg \min E \quad (13)$$

Since the data points are represented as discrete table columns when interpolating, the minimization function is rewritten as

$$Z(x, y) = \sum_{i=1}^n c_i \varphi(\|x - x_i, y - y_i\|) + b_0 + b_1 x + b_2 y \quad (14)$$

where $\|\cdot\|$ is Euclidean distance, c_i is coefficient and φ is a kernel function of TPS with a value of

$$\varphi(r) = r^2 \log(r) \quad (15)$$

$$r_i = (x - x_i)^2 + (y - y_i)^2 \quad (16)$$

According to the algorithm mentioned above, three columns of XYZ data are converted into matrix format, the Thin Plate Spline interpolation method is used to divide mesh, and a smooth 3-D surface can be finally obtained.

3.4. Detection Results and Discussions

From 28 December 2020 to 14 January 2021, drilling cutting was performed nearly every day, with the exception on 13 January 2021 due to mechanical failure of drilling equipment. During this period, the working face advanced 69.25 m and experienced three times of the lower roof weighting and three times of the upper roof weighting. The upper roof weighting compelled lower roof weighting together. The drilling cuttings amount per meter in different drilling lengths was obtained according to the above steps. Due to serious breakage near the coal wall, which made a large error, the cuttings ranging from 0 m to 1 m in the borehole were not taken into account. The detection trails were divided into three stages according to upper roof weighting.

3.4.1. Detection Results

Stage #1

As mentioned above, detections began on 29 December 2020, when the coalface advanced 1661 m, while the roof was in the period of no-weighting. The detecting results showed that the stress concentration zone appeared ahead of the coalface in the range from 9 to 14 m; the cuttings amount was 2.8–3.4 kg/m (Figure 8a). After the coalface advanced 4 m on 30 December 2020, a stress concentration zone indicated by drilling cuttings of 2.6–3.0 kg/m appeared in the range of 10–30 m ahead and 9–13 m laterally; another concentration zone indicated by drilling cuttings 3.0 kg/m appeared in the range of 15–45 m ahead and 13 m laterally (Figure 8b). On 31 December 2020, after the coalface advanced 4 m again, a stress concentration zone indicated by cuttings amount of 2.6–3.0 kg/m appeared in the range of 15–45 m ahead and 9–14 m laterally, and a multi-peak concentration zone appeared at 45 m ahead and 13 m laterally; the maximum cuttings amount was 3.4 kg/m (Figure 8c). On 1 January 2021, after a further 3.75 m coalface advance, a multi-peak

stress concentration zone appeared in the range of 15–45 m ahead and 7–14 m laterally; the maximum cuttings amount of 3.2 kg/m appeared (Figure 8d). On 2 January 2021, a multi-peak stress concentration zone appeared in the range of 5–15 m ahead and 10–14 m laterally, the maximum cuttings amount of 3.5 kg/m appeared (Figure 8e), and the lower roof weighting began with a periodic span of 15.75 m.

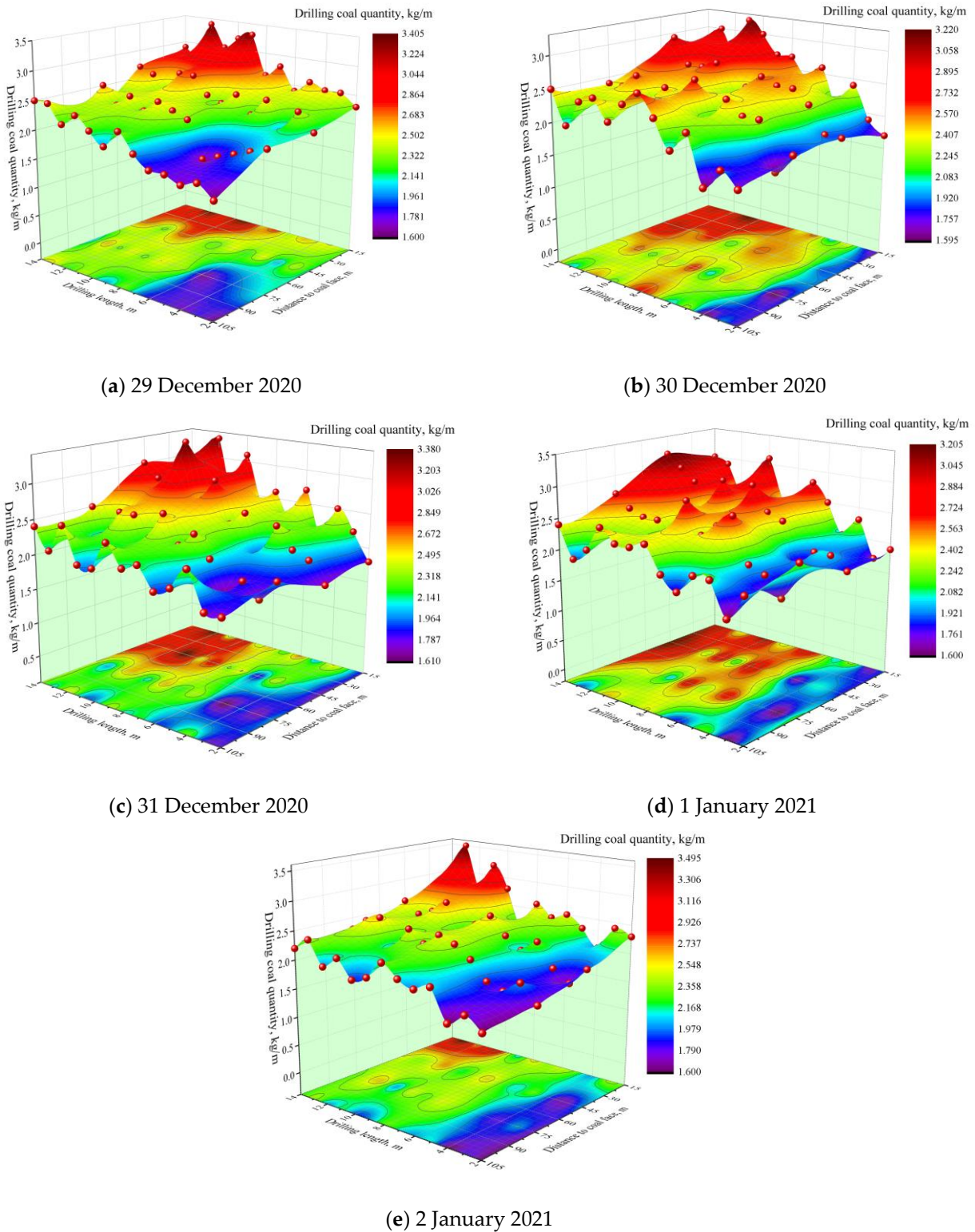


Figure 8. Detection results of stage #1 lower roof weighting.

On 3 January 2021, further 3.75 m coalface advanced after the lower roof weighting, a multi-peak stress concentration zone appeared in the range of 5–15 m ahead and 9–14 m laterally, and the maximum cuttings amount of 4.0 kg/m was reached (Figure 9a). On 4 January 2021, multi-peak stress concentration areas appeared in the range of 20–45 m ahead and 8–13 m laterally and in the range of 60–75 m ahead and 11–14 m laterally. The maximum cuttings amount of 4.2 kg/m was reached (Figure 9b), the upper roof weighting compelled lower roof weighting began together with a periodic span of 15.75 m.

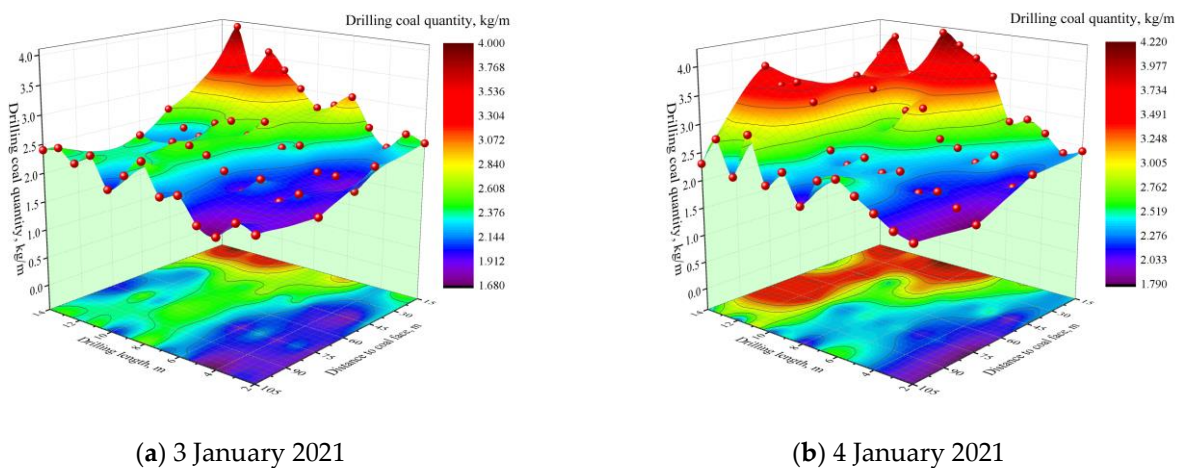


Figure 9. Detection results of stage #1 upper roof weighting.

Stage #2

On 5 January 2021, the coalface advanced 3.75 m after stage #1 roof weighting was completed, a multi-peak stress concentration zone appeared in the range of 5–15 m ahead and 6–14 m laterally, and the maximum cuttings amount of 4.1 kg/m was reached; in the range of 30–45 m ahead and 12–13 m laterally, the maximum cuttings amount of 3.2 kg/m was reached (Figure 10a). On 6 January 2021, the coalface advanced 4 m continuously, multi-peak stress concentration areas formed in the range of 5–15 m ahead and 7–14 m laterally and in the range of 50–75 m ahead and 10–13 m laterally. The maximum cuttings amount of 4.5 kg/m was reached (Figure 10b). On 7 January 2021, after the coalface advanced 4 m, a stress concentration zone appeared in the range of 5–15 m ahead and 11–14 m laterally, the maximum cuttings amount of 3.3 kg/m appeared (Figure 10c), and the lower roof weighting began with a periodic span of 11.75 m.

On 8 January 2021, the coalface advanced a further 3.85 m after the lower roof weighting, a multi-peak stress concentration zone appeared in the range of 15–45 m ahead and 10–14 m laterally, and the maximum cuttings amount of 3.1 kg/m was reached (Figure 11a). On 9 January 2021, after the coalface advanced 4 m, double-peak stress concentration zones appeared in the range of 10–15 m ahead and 10–14 m laterally. The maximum cuttings amount of 4.2 kg/m was reached (Figure 11b). On 10 January 2021, after the coalface advanced 5.4 m, a multi-peak stress concentration zone appeared in the range of 8–15 m ahead and 5–14 m laterally. The maximum cuttings amount of 3.4 kg/m was reached (Figure 11c). Then, the upper roof weighting compelled lower roof weighting began together with a periodic span of 25 m.

Stage #3

On 11 January 2021, the coalface advanced 5.25 m after stage #2 roof weighting was completed, a multi-peak stress concentration zone appeared in the range of 15–75 m ahead and 5–14 m laterally, and the maximum cuttings amount of 4.3 kg/m was reached (Figure 12a). On 12 January 2021, the coalface advanced 5.25 m continuously, a stress concentration area formed in the range of 15–45 m ahead and 11–14 m laterally, and the

maximum cuttings amount of 4.2 kg/m was reached (Figure 12b). Then, the lower roof weighting began with a periodic span of 10.5 m.

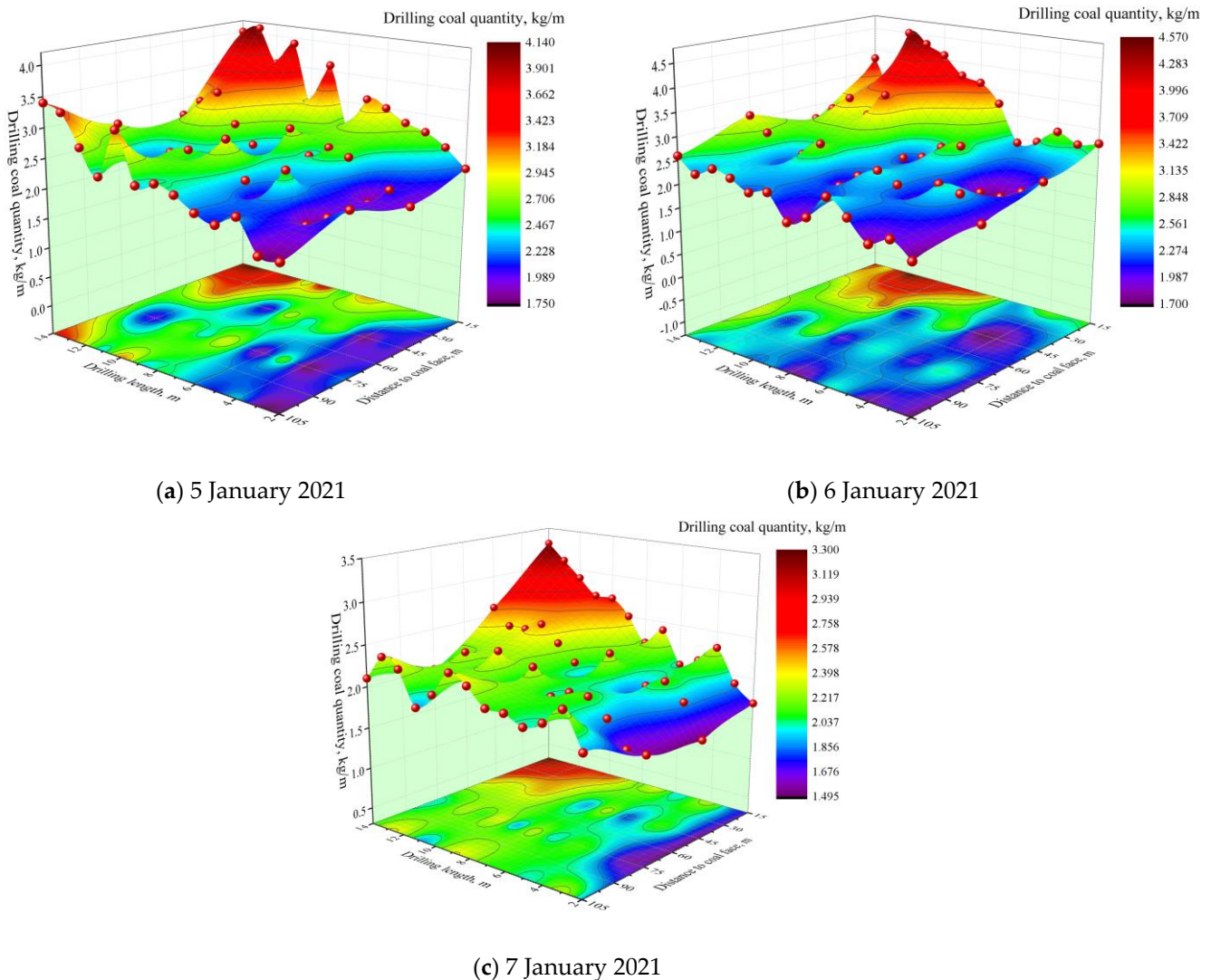
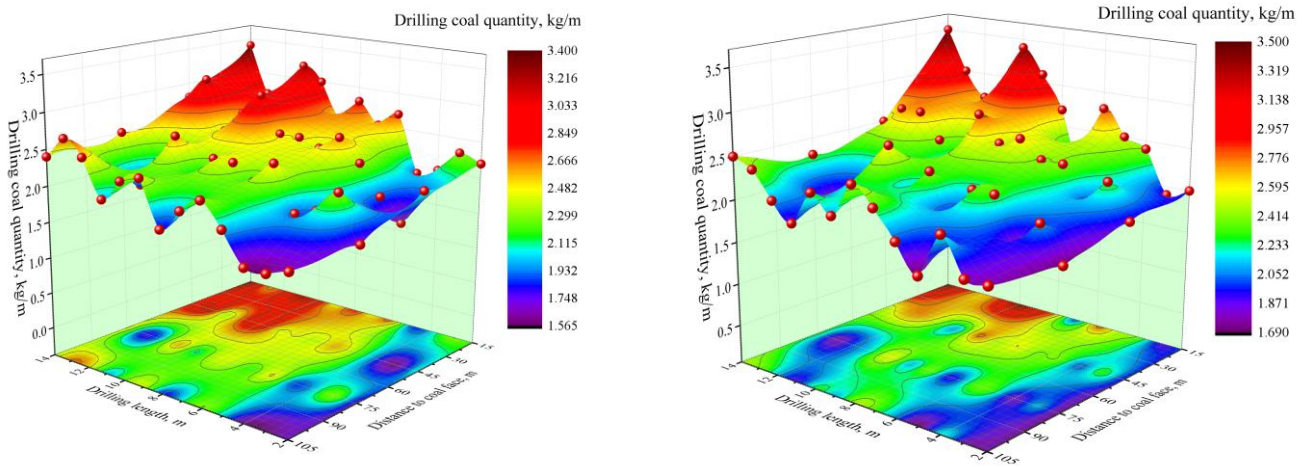


Figure 10. Detection results of stage #2 lower roof weighting.

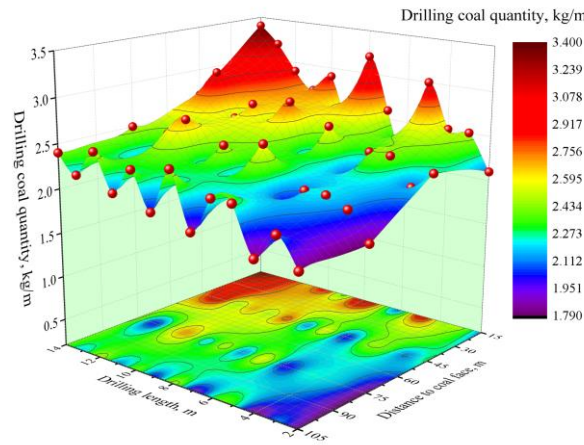
On 13 January 2021, the coalface advanced 5.25 m further after the lower roof weighting; no detection was performed because the drilling machine was incorrect. On 14 January 2021, after the coalface advanced 5.25 m again, a multi-peak stress concentration zone appeared in the range of 15–45 m ahead and 6–14 m laterally. The maximum cuttings amount of 3.5 kg/m was reached (Figure 13). Then, the upper roof weighting compelled lower roof weighting began together with a periodic span of 21 m.

To sum up, the average weighting span of the three times of lower roof weighting alone and three times of upper roof weighting (forced lower roof weighting together) are 12.67 m and 23.1 m, separately. It must be implemented that the determination of roof weighting was verified by the variation of the working resistance of supports in working face. The results showed that the average resistance of supports is 6340 KN in the no-weighting stage of roof, and the average resistance of supports is 7336 KN in the roof weighting stage. The ratio of the latter to the former, i.e., the weighting factor, is 1.16.



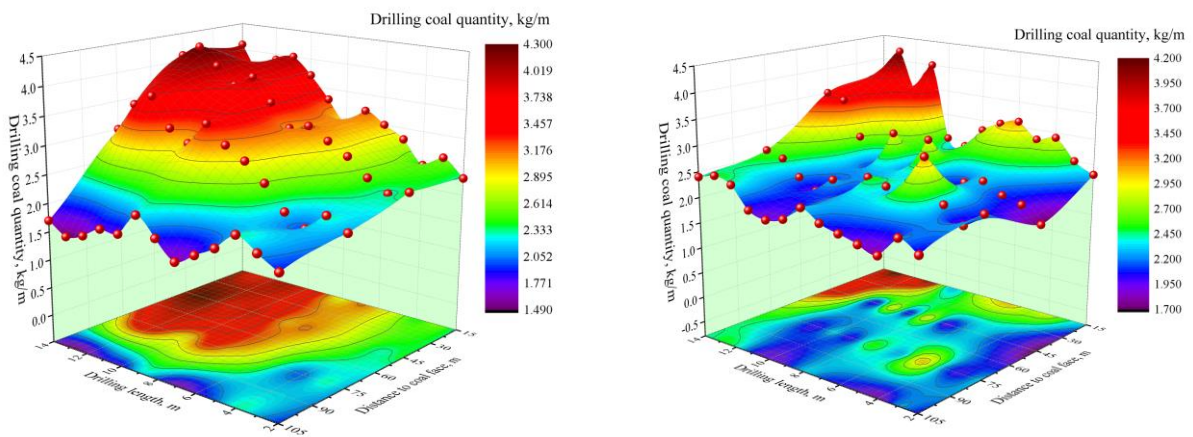
(a) 8 January 2021

(b) 9 January 2021



(c) 10 January 2021

Figure 11. Detection results of stage #2 upper roof weighting.



(a) 11 January 2021

(b) 12 January 2021

Figure 12. Detection results of stage #3 lower roof weighting.

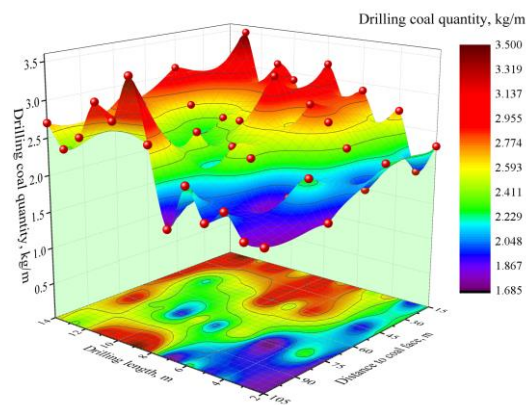


Figure 13. Detection results of stage #3 upper roof weighting.

3.4.2. Discussions

The variation of drilling cuttings has good correspondence with roof movement and weighting. The drilling cuttings amount reflects the different layers of roof strata. In this investigation, when the lower roof is active, the concentration range of drilling cuttings is relatively narrow, usually about 15–45 m. When the upper roof is active, the lower roof will be forced to break off and move together; its corresponding drilling cuttings concentration range is relatively large, up to 45–75 m. Therefore, through detecting the variation of the concentrated area of drilling cuttings, the pattern of variation can be obtained, which can be used to predict the weighting and its influence range.

The results of drilling cuttings detection showed that, with the change of coalface advances, stress concentration zones can be identified in general. Especially, the heterogeneity and fluctuation of stress concentration can be mapped. As matter of fact, the coal seam is uneven, and the regional characteristics are obvious, which is due to the uneven distribution of joints and fractures in different scales in the coal seam. As the coalface advances, in addition, the change of abutment pressure leads to the uneven damage and destruction of the area, which causes the obvious non-uniformity of stress concentration and the “multi-region” appearance. This investigation breaks the previous understanding of homogenizing the mining-induced stress concentration area. Thus, it is very important to obtain the stress concentration area based on the inhomogeneity of the defects in the coal seam, in order to meet the need of accurate pressure relief in rock burst prevention.

At present, vibration wave detection and online stress monitoring methods are the regular methods for rock burst early warning in some coal mines in China. However, a lot of trials showed vibration wave detection accuracy is limited by penetration distance. Online stress monitoring accuracy is limited by the low number of sensors installed. Generally, there are two sensors installed in one station: the near sensor is only 5 m deep and the far sensor is only 10 m deep, along the horizontal direction of the coal seam. In addition, the stiffness matching between sensor and fractured rock or coal is another factor. Thus, drilling cutting is an indispensable method for rock burst early warning. The description revised as “the detection accuracy of abutment pressure and its changes by using vibration wave detection and online stress monitoring” should be improved

How much influence does the fracture and fault structure of different scales have on the concentration and distribution of stress due to extraction of the coal seam? How can you get close to the actual result through the detection method? These are important issues that need to be addressed. At present, the results of numerical simulation are mainly used as the basis of cognition. However, from the drilling cutting results, the characteristics of stress concentration aroused by extraction are far beyond the previous understanding. Drilling cutting may be an effective approach to obtain the influence of different scale fractures or faults on stress concentration patterns.

It should be noted that the large spacing and short length of boreholes affected the accuracy of results in this investigation. For the detection of pressure concentration and the

prediction of roof weighting, the length and spacing of boreholes have a great influence, and the borehole arrangement should satisfy the engineering needs.

4. Conclusions

Through tests of variation of drilling cuttings amount with different movement stages of the roof, which was performed in Xinglongzhuang Coal Mine, the following conclusions are obtained.

1. The amount of drilling cuttings is related to the stress state as well as the damage degree of the coal seam. It was found that the amount of cuttings drilled is positively related to the degree of stress concentration in both the plastic fracture zone and elastic zone. Thus, drilling cuttings can be taken as an indication for verifying the distribution of abutment pressure and are helpful for pressure relief in mines.
2. The amount of drilling cuttings is closely related to the roof weighting; that is, the stress concentration range is small in the roof stationary stage or the lower roof movement stage, generally in the range of 15 m to 45 m; while in the upper roof movement stage, the stress concentration range is relatively large, which can reach the range of 45 m to 75 m, which also can be utilized for the forecasting of roof weighting.
3. The investigations have shown that the distribution of stress concentration has a fluctuation pattern because of the non-uniformity of cracks and other defects in the coal seam. Thus, there must be enough boreholes to cover the cared area, and optimizing layout is necessary in order to meet the need of accurate pressure relief in rock burst prevention. Although the Thin Plate Spline can be utilized to analyze cutting data, how to distinguish the inhomogeneous distribution of the coal seam by drilling cuttings is further research work in the future.
4. It must be pointed out that using drilling cuttings is only suitable for dry coal seams. For the wet or watery coal seam, some other new effective detection ways should be trialed.

Author Contributions: Conceptualization, J.T.; methodology, J.T. and Y.T.; software, Y.Z.; validation, Y.Z.; formal analysis, Z.W.; investigation, J.T. and Y.T.; resources, Y.T.; data curation, J.T.; writing—original draft preparation, J.T.; writing—review and editing, Y.T.; visualization, Y.Z.; supervision, Y.T.; project administration, Y.T.; funding acquisition, Y.T. All authors have read and agreed to the published version of the manuscript.

Funding: This research was funded by National Natural Science Foundation of China, grant number 52074168 and 51874190.

Institutional Review Board Statement: This study did not involve humans or animals.

Data Availability Statement: This study did not report any data.

Acknowledgments: This work was supported by National Natural Science Foundation of China (52074168, 51874190), and all authors agree it.

Conflicts of Interest: The authors declare no conflict of interest.

References

1. Shuancheng, G.; Chaofan, Y.; Pan, W.; Hongxin, N. Distribution law of supporting pressure and plastic zone of coal pillar in longwall mining. *Sci. Technol. Eng.* **2021**, *21*, 4875–4881. (In Chinese)
2. Enjun, F.; Shuwen, W.; Laiyang, S.; Lingfu, Z.; Lei, Z. Practices on seismic CT technology to detect pilot support pressure distribution of coal mining face. *Coal Eng.* **2011**, *7*, 39–41. (In Chinese)
3. Dechao, W.; Qi, W.; Shucui, L.; Fuqi, W.; Nianbo, G.; Baoqi, W.; Xiangbo, C.; Rui, P. Stress distribution characteristics of deep mine in fully-mechanized sublevel caving face based on microseismic and online stress monitoring system. *J. Min. Saf. Eng.* **2015**, *32*, 382–386. (In Chinese)
4. Mengtao, Z.; Benjun, Z.; Zenghe, X.; Yishan, P. Application of drilling method to estimation of stresses in loosened and broken rock. *J. Fuxin Min. Inst.* **1988**, *7*, 1–8. (In Chinese)
5. Petuhov, I.M. Rock Burst In Coal Mine. *Coal Industry Press.* **1980**, 85–91. (In Chinese)

6. Bo, L.; Benjun, Z.; Jingyi, H. Trial code for rock burst dangerous coal seam in Longfeng Mine of Fushun Mining Bureau. *J. Fuxing Min. Insititute* **1985**, (Sup), 38–42. (In Chinese)
7. Benjun, Z. Studies on coal burst prevention and control in Longfeng Mine, Fushun. *Chin. J. Rock Mech. Eng.* **1987**, *6*, 30–38. (In Chinese)
8. Yishan, P.; Qingxin, Q.; Zhonghua, L.; Jupeng, T.; Linming, D.; Jinhai, L.; Junfeng, P.; Shankun, Z.; Guanghui, Z.; Shaohong, L. Methods for Test, Monitoring and Prevention of Rock Burst—Part 6: Monitoring Method of Drilling Bits. *China National Standasrd: GB/T 25217.6-2019*. **2019**, 1–14. (In Chinese)
9. Xiaocheng, Q.; Fuxing, J.; Zhengxing, Y.; Hongyang, J. Rock burst monitoring and precaution technology based on equivalent drilling research and its applications. *Chin. J. Rock Mech. Eng.* **2011**, *30*, 2346–2351. (In Chinese)
10. Xiangyou, G.; Youlin, X.; Xuyi, M.; Zhongming, Y. Application of the value of drilling cuttings weight and desorption index for drill cuttings to preventing coal and gas outburst. *J. Univ. Sci. Technol. Beijing* **2009**, *31*, 285–289. (In Chinese)
11. Feng, C.; Yihan, P.; Zhonghua, L.; Aiwen, W.; Zhi, T. Detection and study of rock burst hazard based on drilling cuttings method. *Chin. J. Geol. Hazard Control*. **2013**, *24*, 116–119. (In Chinese)
12. Zhen, W.; Xianzheng, M.; Yongjiang, Z. Application of drilling cuttings increment index in disaster prediction of large mining depth and high gas coalmine. *Saf. Coal Mines* **2011**, *42*, 89–92. (In Chinese)
13. Jingda, L.; Quande, W.; Mingkui, J. Method of diameter drilling cuttings inspection and its application. *Saf. Coal Mines* **2016**, *47*, 126–129. (In Chinese)
14. Wang, C.; Li, X.; Xu, C.; Niu, Y.; Chen, Y.; Yang, S.; Zhou, B.; Jiang, C. Study on factors influencing and the critical value of the drilling cuttings weight: An index for outburst risk prediction. *Process. Saf. Environ. Prot.* **2020**, *140*, 356–366. [[CrossRef](#)]
15. Feng, C.; Yishan, P.; Zhonghua, L.; Aiwen, W.; Lianman, X. Analysis and evaluation of effects of borehole pressure relief measures by drilling cutting method. *Chin. J. Geotech. Eng.* **2013**, *35*, 266–270. (In Chinese)
16. Skoczylas, N.; Dutka, B.; Sobczyk, J. Mechanical and gaseous properties of coal briquettes in terms of outburst risk. *Fuel* **2014**, *134*, 45–52. [[CrossRef](#)]
17. Sobczyk, J. The influence of sorption processes on gas stresses leading to the coal and gas outburst in the laboratory conditions. *Fuel* **2011**, *90*, 1018–1023. [[CrossRef](#)]
18. Karakus, M.; Perez, S. Acoustic emission analysis for rock–bit interactions in impregnated diamond core drilling. *Int. J. Rock Mech. Min. Sci.* **2014**, *68*, 36–43. [[CrossRef](#)]
19. Jung, S.J.; Prisbrey, K.; Wu, G. Prediction of rock hardness and drill ability using acoustic emission signatures during indentation. *International J. Rock Mech. Min. Sci.* **1994**, *31*, 561–567. [[CrossRef](#)]
20. Yangsheng, Z.; Cunsheng, L.; Chengdan, L. Exploration of drilling cuttings method for measuring surrounding rock pressure. *Chin. J. Geotech. Eng.* **1987**, *9*, 104–110. (In Chinese)
21. Jupeng, T.; Weijun, L.; Yishan, P.; Shuai, C.; Jiahui, D. Experimental study on the influence of drill pipe diameter and drilling velocity on drilling cuttings. *J. Min. Saf. Eng.* **2019**, *36*, 166–174. (In Chinese)
22. Guangzhi, Y.; Xiaoquan, L.; Hongbao, Z.; Xiaoshuang, L.; Gaoshuai, L. In-situ experimental study on the relation of drilling cuttings weight to ground pressure and gas pressure. *J. Univ. Sci. Technol. Beijing* **2010**, *32*, 1–7. (In Chinese)